# SPECIAL ISSUE ARTICLE



Check for updates

# Influence of oxygen vacancies on the domain wall stability in BiFeO<sub>3</sub>

Mao-Hua Zhang<sup>1</sup> Vueze Tan<sup>1</sup> Tiannan Yang<sup>1,2</sup> Long-Qing Chen<sup>1</sup>

<sup>1</sup>Department of Materials Science and Engineering, The Pennsylvania State University, University Park, Pennsylvania, USA

<sup>2</sup>Interdisciplinary Research Centre, School of Mechanical Engineering, Shanghai Jiao Tong University, Shanghai, China

#### Correspondence

Tiannan Yang and Long-Qing Chen, Department of Materials Science and Engineering, The Pennsylvania State University, University Park, PA 16802, USA.

Email: tuy123@psu.edu and lqc3@psu.edu

### Funding information

US Department of Energy, Office of Science, Basic Energy Sciences, Grant/Award Number: DE-SC0020145; Penn State Center for Nanoscale Sciences, Grant/Award Number: DMR-2011839

### **Abstract**

Oxygen vacancy is the most common type of point defects in functional oxides, and it is known to have profound influence on their properties. This is particularly true for ferroelectric oxides since their interaction with ferroelectric polarization often dictates the ferroelectric responses. Here, we study the influence of the concentration of oxygen vacancies on the stability of ferroelectric domain walls (DWs) in BiFeO<sub>3</sub>, a material with a relatively narrow bandgap among all perovskite oxides, which enables strong interactions among electronic charge carriers, oxygen vacancies, and ferroelectric domains. It is found that the electronic charge carriers in the absence of oxygen vacancies have essentially no influence on the spatial polarization distribution of the DWs due to their low concentrations. Upon increasing the concentration of oxygen vacancies, chargeneutral DWs with an originally symmetric polarization distribution symmetric around the center of the wall can develop a strong asymmetry of the polarization field, which is mediated by the electrostatic interaction between polarization and electrons from the ionization of oxygen vacancies. Strongly charged headto-head DWs that are unstable without oxygen vacancies can be energetically stabilized in the off-stoichiometric BiFeO<sub>3- $\delta$ </sub> with  $\delta \sim 0.02$  where ionization of oxygen vacancies provides sufficient free electrons to compensate the bound charge at the wall. Our results delineate the electrostatic coupling of the ionic defects and the associated free electronic charge carriers with the bound charge in the vicinity of neutral and charged DWs in perovskite ferroelectrics.

#### KEYWORDS

charge compensation, charged domain walls, electronic charge carriers, oxygen vacancy, phase-field simulations

## 1 | INTRODUCTION

J Am Ceram Soc. 2024;1-7.

Ferroelectric oxides are found in many applications, and their functionalities are closely related to the domain structures and behavior of domain walls (DWs).<sup>1–5</sup> Ferroelectric DWs are interfaces that separate uniformly polarized ferroelectric domains with different polarization orientations. DWs can be either electrically neutral or

This is an open access article under the terms of the Creative Commons Attribution License, which permits use, distribution and reproduction in any medium, provided the original work is properly cited.

© 2024 The Authors. Journal of the American Ceramic Society published by Wiley Periodicals LLC on behalf of American Ceramic Society.

wileyonlinelibrary.com/journal/jace

charged, and the formation of DWs is the result of energy minimization. In particular, the electrostatic compatibility of DWs states that the polarization components normal to the DWs are continuous across the walls as an energetically preferred condition, corresponding to charge-neutral DWs with minimized electrostatic energy. Nevertheless, if the bound charge is compensated by free charge carriers and/or charged defects, charged DWs can be stabilized, as has been experimentally established in various material systems. 7–10

Oxygen vacancy is one of the most common point defects in ferroelectric oxides and plays an important role in determining their functionalities. For example, acceptor doping and associated DW pinning by oxygen vacancies has been demonstrated as a common approach to improve the mechanical quality factor for high-power applications. 11,12 In addition, it has been suggested that oxygen vacancy is crucial for the stabilization of the metastable ferroelectric phase in hafnium oxide. 13,14 Previous experimental characterizations have shown the accumulation of oxygen vacancies in the vicinity of charged DWs. 9,15-17 Moreover, it has been found that the local conductivity at DWs can be tailored by controlling the oxygen partial pressure during the preparation of materials, 9,16 indicating the crucial role of oxygen vacancies in electronic conduction at DWs. 18,19 These studies suggest an intimate electrostatic coupling between oxygen vacancies and charged DWs.

Theoretical studies have been carried out to understand the formation of charged DWs. For example, it was reported that charged DWs can be stabilized by the insertion of layers containing charged impurities.<sup>20</sup> In addition, it was suggested that both head-to-head and tail-to-tail configurations are energetically more favorable than the monodomain state of the ferroelectric if the surface polarization effect is strong enough.<sup>21</sup> Furthermore, the screening charge distribution across charged DWs for uniaxial ferroelectrics was investigated.<sup>22</sup> Phasefield methods are widely used for the study of domain structures in ferroelectrics.<sup>23–29</sup> The interaction between domain structures and oxygen vacancies was addressed in a few previous studies.<sup>30</sup> Sluka et al.<sup>8</sup> and Zuo et al.<sup>31,32</sup> assumed a priori the concentration of oxygen vacancies and studied the effect of extrinsic space charges on domain properties in BaTiO3. However, it is unclear whether intrinsic electronic charge carriers can affect ferroelectric domain configurations, at what concentration extrinsic charge carriers begin to play a role in DWs, and whether they can stabilize charged DWs.

Existing phase-field models have been developed mainly for understanding microstructure evolution, and free electrons and holes as degrees of freedom are usually neglected.<sup>25</sup> In this paper, based on a newly developed phase-field framework for modeling coupled electronic and structural processes,<sup>33</sup> we present four case studies of the effect of intrinsic charge carriers and extrinsic ones due to the presence of oxygen vacancies on the domain structures to address the above open questions. We chose BiFeO<sub>3</sub> as an example, which has a band gap of 2.5 eV,<sup>34</sup> one of the narrowest among ferroelectric perovskite oxides, where strong interactions between electronic charge carriers, oxygen vacancies, and ferroelectric domains are expected.

### 2 | METHODS

To model the effect of nonstoichiometry due to the presence of oxygen vacancies on the DW stability in BiFeO<sub>3</sub>, we introduce a set of basic variables, including the spontaneous polarization  $P_i$ , electric potential  $\Phi$ , mechanical displacement  $u_i$ , oxygen vacancy concentration  $[V_O^*]$ , free electron concentration n, and electron hole concentration  $p.^{33}$  For simplicity, we assume that the oxygen vacancy concentration is uniform throughout the system and neglect possible segregation due to the formation energy and volume differences between oxygen vacancies at the DWs and those inside domains. The initial electron and hole concentrations are estimated by assuming complete ionization of oxygen vacancies and Brower approximation,  $n_0 \approx 2[V_O^*]$  where  $n_0$  is the density of free electrons.

We simply use the following time-dependent Ginzburg–Landau equation to relax the spontaneous polarization distribution to an equilibrium<sup>35</sup>:

$$\frac{\partial P_i}{\partial t} = -L \frac{\delta F}{\delta P_i} \tag{1}$$

where t is the time, L is the kinetic coefficient with its inverse related to polarization relaxation constant, and F is the total free energy of the system which includes contributions from bulk chemical free energy density, gradient energy, the electrostatic energy, and the elastic energy.<sup>35</sup> The full set of material coefficients employed for the simulations and a detailed description of the boundary conditions can be found in Table S1 and Supporting Information Note 1. The elastic energy is obtained by solving the mechanical equilibrium equation for displacement  $u_i$  with the eigenstrain distribution determined by the electrostrictive effect. The electric potential and thus the electric field distribution are determined by solving the electrostatic Poisson equation using the background dielectric constant with the total local charge density containing contributions from oxygen vacancies, free electrons, electron holes as well as the bound polarization charge.

The interaction between domain structures and electronic charge density  $\rho$  is governed by the electrostatic Poisson equation:

$$\nabla \cdot (-\kappa_0 \kappa^b \nabla \Phi + \mathbf{P}) = e(p - n) + \rho_{\text{defects}} \tag{2}$$

where  $\kappa_0$  and  $\kappa^b$  are the vacuum permittivity and background dielectric permittivity, respectively, e and p are electron and electron hole concentrations, and  $\rho_{\text{defects}}$  is the free charge contributed from charge defects.

The spatial distributions of the electron and hole concentrations are obtained by evolving the electron/hole transport equations until an equilibrium:

$$\frac{\partial n}{\partial t} = -\nabla \cdot \mathbf{j}_e + R \tag{3}$$

$$\frac{\partial p}{\partial t} = -\nabla \cdot \mathbf{j}_h + R \tag{4}$$

where R is the net generation rate of electron-hole pairs including electron-hole creation and recombination and is zero at equilibrium, and  $\mathbf{j}_e$  and  $\mathbf{j}_h$  are the flux densities of free electrons and holes, respectively.

In addition, the elastic equilibrium condition is satisfied:

$$\frac{\partial \sigma_{ij}}{\partial x_i} = 0 \tag{5}$$

where  $\sigma_{ij}$  is the elastic stress. For more details of all the expressions for the free energy density function, mechanical equilibrium equation, and electrostatic equilibrium equation, we refer to Yang and Chen.<sup>33</sup>

### 3 | RESULTS AND DISCUSSION

# 3.1 | Charge-neutral DWs without oxygen vacancies

One-dimensional (1D) simulations were carried out for studying the stability of the ferroelectric domain structures with a system size of 64 nm, which is discretized into 256 grids. We first examine charge-neutral 109° DWs to investigate the effect of intrinsic (i.e., thermally activated) charge carriers on the domain structures without introducing oxygen vacancies, as shown in Figure 1A. Our results show that the electronic carriers have no significant effect on the polarization profiles, as can be seen in Figure 1B, where the peaks of polarization at x = 16 nm and x = 48 nm mark the positions of the DWs. They also have negligible effect on the electric potential (Figure 1C) and the bound charge density (Figure 1D). This is due to the extremely low concentration of intrinsic electrons and holes ( $\sim 10^6 \text{ m}^{-3}$ ) and hence, the electronic charge density ( $\sim 10^{-13} \text{ C/m}^3$ ) is orders of magnitude lower than the polarization bound

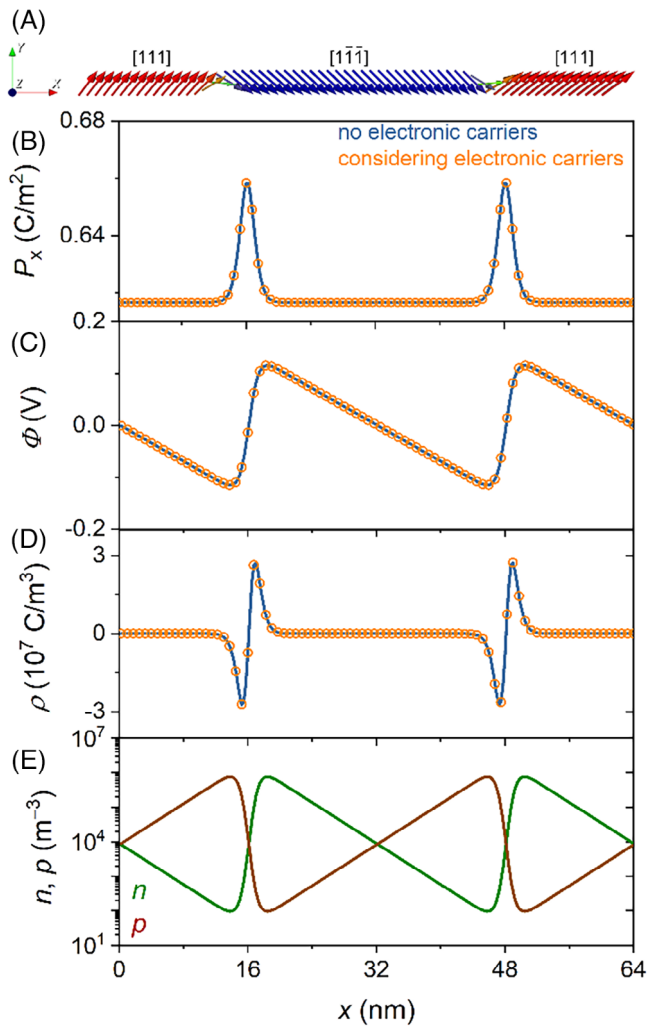


FIGURE 1 (A) Schematic of the simulated charge-neutral  $109^{\circ}$  domains, (B) polarization along the x direction,  $P_x$ , (C) electric potential, (D) bound charge density, and (E) electron and hole concentrations of the charge-neutral  $109^{\circ}$  DWs with (in green) and without (in brown) consideration of intrinsic charge carriers without introduction of oxygen vacancies. DWs, domain walls.

charge density ( $\sim 10^7$  C/m<sup>3</sup>) in the modeled DW system. As a result, the interaction between charge carriers and ferroelectric polarization is minimal and thus imposes a negligible effect on the stability and the polarization profile of the DW.

An electric potential difference of 0.35 V across the DWs is comparable to other reported values of 0.45 V in  $BaTiO_3^{30}$  and 0.18 V in  $PbTiO_3^{36}$ . The electrons and holes are attracted to the two sides of the DWs due to the electric fields, as illustrated in Figure 1E. Since the divergence of the polarization along the x direction has opposite signs, a negative and a positive bound charge (expressed as  $\rho = -\nabla \cdot P$ ) is observed on the left and right side of the DWs, respectively. Intrinsic charge carriers also have negligible influence on the polarization profiles, the electric potential, and the bound charge density of 71° DWs, as shown in Figure S1.

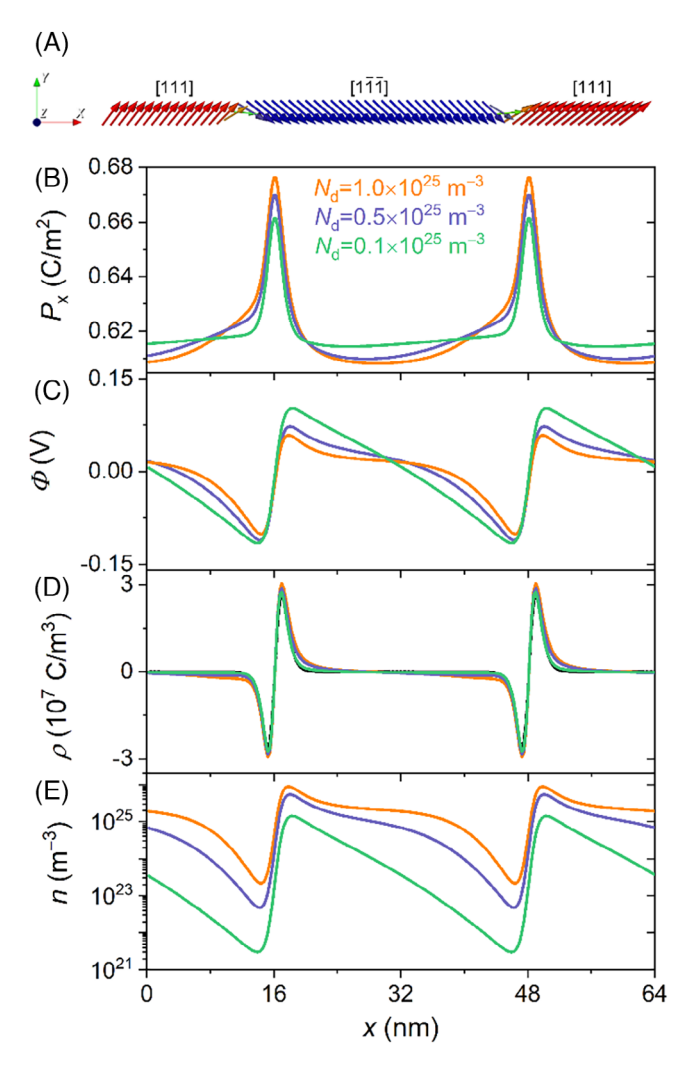


FIGURE 2 (A) Schematic of the simulated uncharged 109° domains, (B) polarization along the x direction, (C) electric potential, (D) bound charge density, and (E) electron concentrations of the uncharged 109° DWs with different concentrations (1  $\times$  10<sup>24</sup>, 5  $\times$  10<sup>24</sup>, and 1  $\times$  10<sup>25</sup> m<sup>-3</sup>) of oxygen vacancies. DWs, domain walls.

# 3.2 | Charge-neutral DWs with oxygen vacancies

Next, we examine the same  $109^{\circ}$  DW systems (illustrated in Figure 2A) but now with certain levels of oxygen vacancies introduced to the material. The equilibrium polarization profiles at several different levels of oxygen vacancy concentration are plotted in Figure 2B. At oxygen vacancy concentrations below  $N_d = 10^{24}$  m<sup>-3</sup>, the simulated polarization profile is very similar to the case with only intrinsic charge carriers, while it becomes significantly different at higher concentrations of oxygen vacancies. This is accompanied by a change in the profiles of the electric potential (Figure 2C), which induces a change in the electric field (Figure S2). At an oxygen vacancy level of  $N_d = 10^{25}$  m<sup>-3</sup>, the magnitude of the average electronic charge density ( $\sim 10^7$  C/m<sup>3</sup>) becomes comparable to the magnitude of the

polarization bound charge ( $\sim 10^7$  C/m<sup>3</sup>). As a result, the profiles of the bound charge have changed, as shown in Figure 2D. High concentrations of electrons are attracted to the right side of the DWs, reaching a maximum density of  $1.20 \times 10^{26} \text{ m}^{-3}$  (Figure 2E). The electron concentration on the left side falls below  $10^{24}$  m<sup>-3</sup> as the sign of the bound charge changes from positive to negative across the DWs. In contrast, the hole concentration is negligible across the DWs within the system dominated by donor-type defects (Figure S3). The asymmetry of the electron concentration profile across the DWs significantly alters the electrostatic potential profile shown in Figure 1C and is thus responsible for the observed formation of the asymmetric DWs (Figure 2B) via the electrostatic interaction between ionic defects and free electronic charge carriers. Note that an electron concentration of  $1 \times 10^{24} \text{ m}^{-3}$  and  $1 \times 10^{25} \text{ m}^{-3}$ corresponds to a nonstoichiometry of  $BiFeO_{3-\delta}$  with  $\delta$  $\sim 0.00012$  and  $\delta \sim 0.00125$ , respectively. Such a degree of oxygen nonstoichiometry is rather common and has been reported both experimentally<sup>37,38</sup> and theoretically<sup>39</sup> in perovskite oxides.

# 3.3 | Strongly charged DWs

We further examine head-to-head and tail-to-tail 109° DWs (illustrated in Figure 3A), which are strongly charged and require charge compensation at both the head-to-head (electrons required) and tail-to-tail (holes required) DWs (Figure 3A) to stabilize. It was found that such domain structures are energetically unstable at an oxygen vacancy concentration of  $1 \times 10^{25}$  m<sup>-3</sup> or lower and thus will transform into a single domain, signifying insufficient charge compensation (Figure S4). When the oxygen vacancy concentration increases to  $N_d = 1.50 \times 10^{26} \text{ m}^{-3}$ , a high bound charge density of  $2.47 \times 10^8$  C/m<sup>3</sup> at the head-to-head DWs can be almost completely compensated by a high local electron concentration of  $1.78 \times 10^{27} \text{ m}^{-3}$  (Figure 3F). As a result, the angle between the domains on both sides of the head-to-head DWs is nearly 109° (Figure 3B). In contrast, the bound charge of tail-to-tail DWs is not sufficiently compensated due to a low concentration of holes ( $\sim 10^{-8} \text{ m}^{-3}$ ) and thus, the angle of the DW deviates significantly from 109°. Moreover, the width of tail-to-tail DWs is significantly broadened, which may help to reduce the magnitude of the bound charge. The extremely high electronic carrier concentration in the vicinity of charged DWs is similar to that found in BaTiO3 with a local electron/hole concentration of  $\sim 10^{25}$  m<sup>-3</sup> as a result of band bending.<sup>40</sup> Here, the donor concentration exceeds the effective density of states of the conduction band ( $\sim 1.33 \times 10^{26} \text{ m}^{-3}$ ), signifying a relocation of the Fermi energy into the conduction band for the head-to-head DWs. In view of the previous study<sup>40</sup> and the present results, it is concluded that

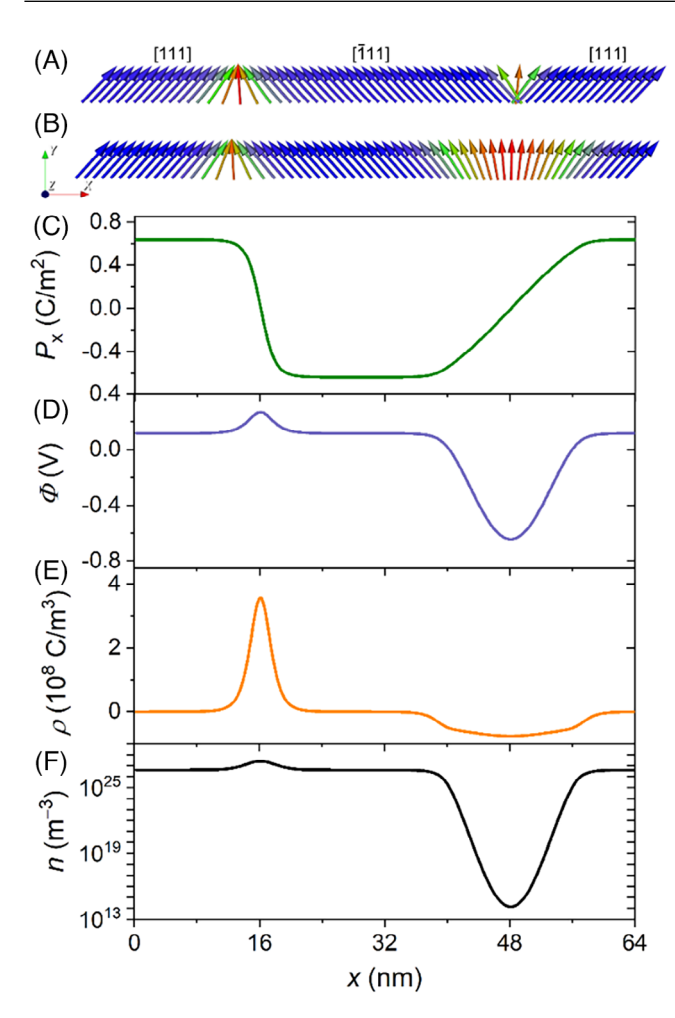


**FIGURE 3** (A) Schematic of the simulated head-to-head and tail-to-tail 109° domains as the initial domain structure and (B) equilibrium domain structure with an oxygen vacancy concentration of  $1.50 \times 10^{26}$  m<sup>-3</sup>, which corresponds to a nonstoichiometry of BiFeO<sub>3- $\delta$ </sub> with  $\delta \sim 0.02$  (C) polarization along the *x* direction, (D) electric potential, (E) bound charge density, and (F) electron concentration of the charged 109° domain structures.

stabilization of head-to-head (tail-to-tail) DWs is not possible without a change in the band structure, since sufficient compensation of such strongly charged DWs cannot be accomplished by the typical concentration of free charge carriers expected in wide-bandgap semiconductors. An oxygen vacancy concentration of 1.50  $\times$  10 $^{26}$  m $^{-3}$  corresponds to a nonstoichiometry of BiFeO $_{3-\delta}$  with  $\delta\sim0.02$  that is experimentally  $^{37,38}$  and theoretically  $^{39}$  possible in perovskite oxides.

# 3.4 | Weakly charged DWs

Head-to-head and tail-to-tail DWs are also referred to as strongly charged DWs because they must be sustained by sufficient charge screening. In comparison, weakly

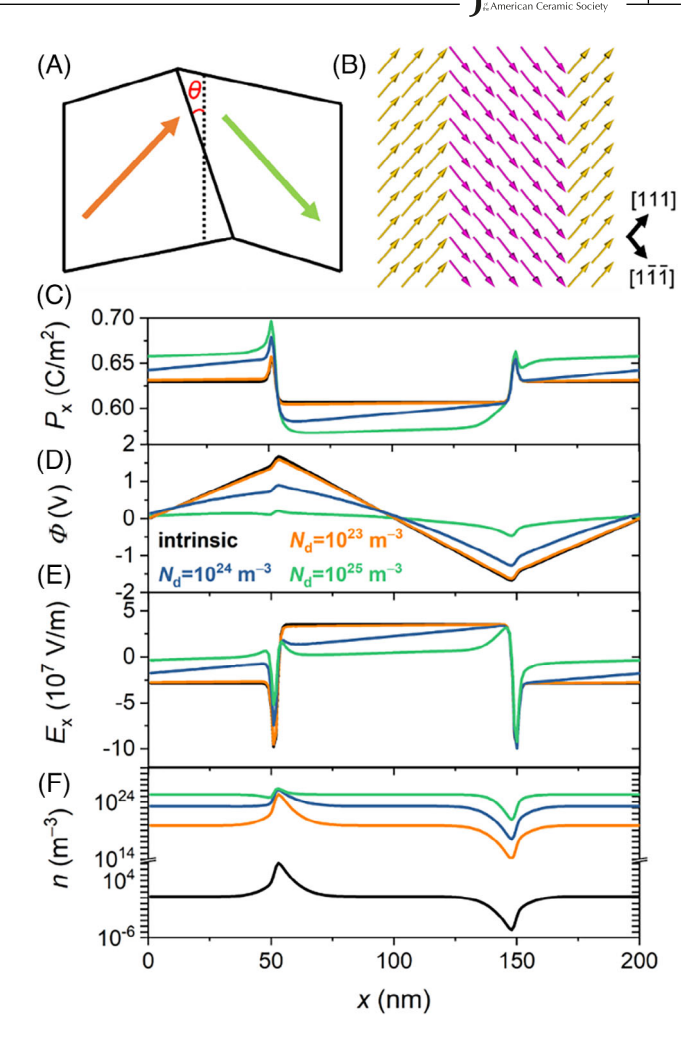


**FIGURE 4** (A) Schematic of 109° weakly charged DWs with a small deviation of 5° from their charge-neutral orientations (shown with dashed lines) and (B) the simulated domain structure. (C) Polarization component along the (100) direction (*x*-axis), (D) electric potential, (E) electric field along the (100) direction, and (F) electron concentration of the weakly charged 109° domain structures with different concentrations (10<sup>23</sup>, 10<sup>24</sup>, and 10<sup>25</sup> m<sup>-3</sup>) of oxygen vacancies.

charged DWs denote DWs with a small deviation from the original charge-neutral orientation, resulting in a nonzero change in the polarization components normal to the DWs,  $^{6,41}$  as illustrated in Figure 4A. To understand the effect of oxygen vacancies on the weakly charged DWs, we take DWs with a tilt angle  $\theta$  of  $5^{\circ}$  in a 200  $\times$  200 nm system, which is discretized into 200  $\times$  200 grids (Figure 4B). The DWs on the left side of Figure 4B is positively charged, while the DW on the right side is negatively charged.

The polarization and bound charge (Figure S5) profiles across the DWs are asymmetric due to the tilt of the DWs and the degree of asymmetry increases with increasing oxygen vacancy concentration, as shown in Figure 4C. The polarization along the *x*-direction in the yellow domain indicated in Figure 4B increases with increasing oxygen

and-conditions) on Wiley Online Library for rules of use; OA articles are governed by the applicable Creative Commons License

vacancy concentration, while it decreases in the purple domain with increasing oxygen vacancy concentration, which can be seen as a slight clockwise rotation of the polarization vectors in the two domains. The increased net polarization component perpendicular to the DWs (representing the surface charge density) is compensated by a larger number of electrons upon increasing oxygen vacancy concentrations (Figure 4F), as demonstrated by a flattening of the electric potential (Figure 4D). However, it is found that the presence of extrinsic charge carriers cannot effectively reduce the total energy of the system (Figure S6). In contrast to strongly charged head-to-head DWs, charge screening is not a must for weakly charged DWs because the bound charge density of the latter ( $\sim 10^7$ C/m<sup>3</sup>) is an order of magnitude smaller than that of the former ( $\sim 10^8$  C/m<sup>3</sup>) and similar to that of the charge-neutral DWs.

### 4 | CONCLUSION

To summarize, we investigate how oxygen vacancies affect the stability of DWs through the electrostatic interaction between the bound charge of ferroelectric domains and the electrons from the ionization of oxygen vacancies. We consider four case studies on the uncharged, strongly charged, and weakly charged DWs in BiFeO<sub>3</sub>. In the absence of oxygen vacancies, electronic carriers in the material hardly change the spatial polarization distribution of charge neutral 109°/71° DWs due to their low concentrations and thus negligible contribution to the local charge density. Introduction of oxygen vacancies boosts the electron concentration and induces asymmetric polarization distribution around the center of the DWs for an oxygen vacancy concentration above  $1 \times 10^{24} \text{ m}^{-3}$ , corresponding to a nonstoichiometry of BiFeO<sub>3- $\delta$ </sub> with  $\delta \sim 0.00012$ . Furthermore, strongly charged head-to-head DWs can be stabilized by an oxygen vacancy concentration of  $1.50 \times 10^{26} \text{ m}^{-3}$  (corresponding to a nonstoichiometry of BiFeO<sub>3- $\delta$ </sub> with  $\delta \sim$ 0.02) or more in synergy with the redistribution of electrons to compensate the high bound charge density, with their pairing tail-to-tail DWs widened as a result of insufficient charge compensation. Note that the current study assumes a uniform distribution of oxygen vacancy. If segregation of oxygen vacancy is considered, a lower oxygen vacancy is required for stabilization of the charged DWs and  $\delta = 0.02$  represents an upper limit of nonstoichiometry. The local bound charge density of weakly charged DWs is comparable to that of charge neutral DWs, which can be stabilized by intrinsic charge carriers. It is concluded that the stabilization of strongly charged DWs by charge compensation of charge carriers is always accompanied by a relocation of the Fermi energy into the conduction

band. The present work provides a concise interpretation of the electrostatic coupling of oxygen vacancies and the associated electronic charge carriers with the ferroelectric DWs in perovskite ferroelectric materials. Since the electrostatic coupling of the ionic defects and the associated free electronic carriers with the polarization bound charge dictates the functionality of perovskite ferroelectrics, our study also points out that we may be able to tune the local conductivity by controlling the charged DWs through the modulation of oxygen vacancies.

### **ACKNOWLEDGMENTS**

The work is supported by the Computational Materials Sciences Program funded by the US Department of Energy, Office of Science, Basic Energy Sciences, under Award Number DE-SC0020145. Y. Tan acknowledges the support from the Penn State Center for Nanoscale Sciences, an NSF MRSEC under the grant number DMR-2011839 (2020–2026). Computations for this research were performed on the Pennsylvania State University's Institute for Computational and Data Sciences' Roar supercomputer.

### ORCID

Mao-Hua Zhang https://orcid.org/0000-0002-9823-4547

### REFERENCES

- Merz WJ. Domain formation and domain wall motions in ferroelectric BaTiO<sub>3</sub> single crystals. Phys Rev. 1954;95(3):690–98.
- Catalan G, Seidel J, Ramesh R, Scott JF. Domain wall nanoelectronics. Rev Mod Phys. 2012;84(1):119–56.
- 3. Nataf GF, Guennou M, Gregg JM, Meier D, Hlinka J, Salje EKH, et al. Domain-wall engineering and topological defects in ferroelectric and ferroelastic materials. Nat Rev Phys. 2020;2(11):634–48.
- Meier D, Selbach SM. Ferroelectric domain walls for nanotechnology. Nat Rev Mat. 2022;7(3):157–73.
- Schultheiß J, Picht G, Wang J, Genenko YA, Chen LQ, Daniels JE, et al. Ferroelectric polycrystals: structural and microstructural levers for property-engineering via domain-wall dynamics. Prog Mater Sci. 2023;136:101101.
- Bednyakov PS, Sturman BI, Sluka T, Tagantsev AK, Yudin PV. Physics and applications of charged domain walls. npj Comput Mater. 2018;4(1):65.
- 7. Seidel J, Martin LW, He Q, Zhan Q, Chu YH, Rother A, et al. Conduction at domain walls in oxide multiferroics. Nat Mater. 2009;8(3):229–34.
- Sluka T, Tagantsev AK, Bednyakov P, Setter N. Free-electron gas at charged domain walls in insulating BaTiO<sub>3</sub>. Nat Commun. 2013;4(1):1808.
- Rojac T, Bencan A, Drazic G, Sakamoto N, Ursic H, Jancar B, et al. Domain-wall conduction in ferroelectric BiFeO<sub>3</sub> controlled by accumulation of charged defects. Nat Mater. 2017;16(3):322– 27.
- Risch F, Tikhonov Y, Lukyanchuk I, Ionescu AM, Stolichnov I. Giant switchable non thermally-activated conduction in

Journal 1 7

- $180^{\circ}$  domain walls in tetragonal Pb(Zr,Ti)O<sub>3</sub>. Nat Commun. 2022;13(1):7239.
- Morozov MI, Damjanovic D. Charge migration in Pb(Zr,Ti)O3 ceramics and its relation to ageing, hardening, and softening. J Appl Phys. 2010;107(3):034106.
- 12. Liu Y-X, Qu W, Thong H-C, Zhang Y, Zhang Y, Yao F-Z, et al. Isolated-oxygen-vacancy hardening in lead-free piezoelectrics. Adv Mater. 2022;34(29):2202558.
- He R, Wu H, Liu S, Liu H, Zhong Z. Ferroelectric structural transition in hafnium oxide induced by charged oxygen vacancies. Phys Rev B. 2021;104(18):L180102.
- Zhou Y, Zhang YK, Yang Q, Jiang J, Fan P, Liao M, et al. The effects of oxygen vacancies on ferroelectric phase transition of HfO<sub>2</sub>-based thin film from first-principle. Comput Mater Sci. 2019;167:143–50.
- Farokhipoor S, Noheda B. Local conductivity and the role of vacancies around twin walls of (001)—BiFeO<sub>3</sub> thin films. J Appl Phys. 2012;112(5):052003.
- Geng WR, Tian XH, Jiang YX, Zhu YL, Tang YL, Wang YJ, et al. Unveiling the pinning behavior of charged domain walls in BiFeO<sub>3</sub> thin films via vacancy defects. Acta Mater. 2020;186:68–76.
- 17. Liu Z, Wang H, Li M, Tao L, Paudel TR, Yu H, et al. Inplane charged domain walls with memristive behaviour in a ferroelectric film. Nature. 2023;613(7945):656–61.
- Seidel J, Maksymovych P, Batra Y, Katan A, Yang SY, He Q, et al. Domain wall conductivity in La-doped BiFeO<sub>3</sub>. Phys Rev Lett. 2010;105(19):197603.
- Petralanda U, Kruse M, Simons H, Olsen T. Oxygen vacancies nucleate charged domain walls in ferroelectrics. Phys Rev Lett. 2021;127(11):117601.
- Wu X, Vanderbilt D. Theory of hypothetical ferroelectric superlattices incorporating head-to-head and tail-to-tail 180° domain walls. Phys Rev B, 2006;73(2):020103.
- Gureev MY, Tagantsev AK, Setter N. Head-to-head and tail-totail 180° domain walls in an isolated ferroelectric. Phys Rev B. 2011;83(18):184104.
- 22. Eliseev EA, Morozovska AN, Svechnikov GS, Gopalan V, Shur VY. Static conductivity of charged domain walls in uniaxial ferroelectric semiconductors. Phys Rev B. 2011;83(23):235313.
- 23. Nambu S, Sagala DA. Domain formation and elastic longrange interaction in ferroelectric perovskites. Phys Rev B. 1994;50(9):5838–47.
- Li YL, Hu SY, Liu ZK, Chen LQ. Phase-field model of domain structures in ferroelectric thin films. Appl Phys Lett. 2001;78(24):3878–80.
- 25. Chen L-Q. Phase-field method of phase transitions/domain structures in ferroelectric thin films: a review. J Am Ceram Soc. 2008;91(6):1835–44.
- 26. Zhang W, Bhattacharya K. A computational model of ferroelectric domains. Part I: model formulation and domain switching. Acta Mater. 2005;53(1):185–98.
- 27. Xu B-X, Schrade D, Gross D, Mueller R. Phase field simulation of domain structures in cracked ferroelectrics. Int J Fract. 2010;165(2):163–73.
- 28. Wang J-J, Wang B, Chen L-Q. Understanding, predicting, and designing ferroelectric domain structures and switching guided

- by the phase-field method. Annu Rev Mater Res. 2019;49(1):127–52.
- Fan L, Werner W, Subotić S, Schneider D, Hinterstein M, Nestler B. Multigrain phase-field simulation in ferroelectrics with phase coexistences: an improved phase-field model. Comput Mater Sci. 2022;203:111056.
- Hong L, Soh AK, Du QG, Li JY. Interaction of O vacancies and domain structures in single crystal BaTiO<sub>3</sub>: two-dimensional ferroelectric model. Phys Rev B. 2008;77(9):094104.
- Zuo Y, Genenko YA, Xu B-X. Charge compensation of headto-head and tail-to-tail domain walls in barium titanate and its influence on conductivity. J Appl Phys. 2014;116(4): 044109.
- Zuo Y, Genenko YA, Klein A, Stein P, Xu B. Domain wall stability in ferroelectrics with space charges. J Appl Phys. 2014;115(8):084110.
- Yang T, Chen L-Q. Dynamical phase-field model of coupled electronic and structural processes. npj Comput Mater. 2022;8(1):130.
- Sando D, Carrétéro C, Grisolia MN, Barthélémy A, Nagarajan V, Bibes M. Revisiting the optical band gap in epitaxial BiFeO<sub>3</sub> thin films. Adv Opt Mater. 2018;6(2):1700836.
- Chen LQ. Phase-field method of phase transitions/domain structures in ferroelectric thin films: a review. J Am Ceram Soc. 2008;91(6):1835–44.
- Meyer B, Vanderbilt D. Ab initio study of ferroelectric domain walls in PbTiO<sub>3</sub>. Phys Rev B. 2002;65(10):104111.
- Aschauer U, Pfenninger R, Selbach SM, Grande T, Spaldin NA. Strain-controlled oxygen vacancy formation and ordering in CaMnO<sub>3</sub>. Phys Rev B. 2013;88(5):054111.
- 38. Inkinen S, Yao L, van Dijken S. Reversible thermal strain control of oxygen vacancy ordering in an epitaxial  $La_{0.5}Sr_{0.5}CoO_{3-\delta}$  film. Phys Rev Mater. 2020;4(4):046002.
- 39. Kotomin EA, Mastrikov YA, Kuklja MM, Merkle R, Roytburd A, Maier J. First principles calculations of oxygen vacancy formation and migration in mixed conducting  $Ba_{0.5}Sr_{0.5}Co_{1-y}Fe_yO_{3-\delta}$  perovskites. Solid State Ionics. 2011;188(1):1–5.
- 40. Sluka T, Tagantsev AK, Damjanovic D, Gureev M, Setter N. Enhanced electromechanical response of ferroelectrics due to charged domain walls. Nat Commun. 2012;3(2):748.
- Seidel J. Topological structures in ferroic materials. Switzerland: Springer International Publishing; 2016.

# SUPPORTING INFORMATION

Additional supporting information can be found online in the Supporting Information section at the end of this article.

How to cite this article: Zhang M-H, Tan Y, Yang T, Chen L-Q. Influence of oxygen vacancies on the domain wall stability in BiFeO<sub>3</sub>. J Am Ceram Soc. 2024;1–7. https://doi.org/10.1111/jace.19752